BOTTOM AND TOP PHYSICS

K. J. Foley*
Brookhaven National Laboratory, Upton, Long Island, NY 11973

A. Fridman
*ELOISATRON Project and Institut National de Physique Nucleaire
et de Physique des Particules, France*

F. J. Gilman[†]
Stanford Linear Accelerator Center, Stanford University, Stanford, CA 94305

G. Herten*
*Department of Physics and Laboratory for Nuclear Science,
Massachusetts Institute of Technology, Cambridge, MA 02139*

I. Hinchliffe[‡]
Lawrence Berkeley Laboratory, University of California, Berkeley, CA 94720

A. Jawahery[◇]
Physics Department, Syracuse University, Syracuse, NY 13210

A. Sanda[○]
Physics Department, Rockefeller University, New York, NY 10021

M. P. Schmidt[△]
Physics Department, Yale University, New Haven, CT 06511

K. R. Schubert
Institut fur Hochenergiephysik, Universitat Heidelberg, Heidelberg, Germany

ABSTRACT

The production of bottom quarks at the SSC and the formalism and phenomenology of observing CP violation in B meson decays is discussed. The production of a heavy t quark which decays into a real W boson, and what we might learn from its decays is examined.

1. Introduction

The physics of heavy flavors promises to be an important component of SSC physics and has been studied intensively in the Snowmass Workshops[1,2] in 1984 and 1986. The production of heavy quark flavors occurs primarily by the strong interactions and offers another arena in which to test QCD and to probe gluon distributions at very small values of x. Such quarks can also be produced as decay products of possible new, yet undiscovered particles, $e.g.$, Higgs bosons, and therefore are a necessary key to reconstructing such particles. The decay products of heavy quarks, especially from their semileptonic decays, can themselves form a background to other new physics processes. Perhaps most important of all, in their rare decays and in CP violating asymmetries formed by studying their weak decays, particles containing heavy quarks can give us further insight into the boundary between what is to be understood inside the standard model and what physics lies beyond.

This is particularly the case with respect to the B meson system. It has been apparent for some time that rare decays and CP violation are especially important to pursue[3] at the SSC where the number of produced B mesons will exceed by many orders of magnitude those produced at any existing or planned colliding beam (but not fixed target) facility. At Snowmass 86, a major development which increased the optimism about doing B physics at the SSC, and that drove much of the discussion in this area, was the success of silicon strip vertex detectors in cleanly extracting charm physics in fixed target experiments. During this past year there was another major development which makes the difficult measurement of a CP asymmetry in B decays much easier (although still very difficult)—the observation of large $B_d^\circ - \overline{B}_d^\circ$ mixing by the ARGUS collaboration.[4]

In the next Section we review the production of b quarks at the SSC, which has an interest of its own from the perspective of QCD. It is also a prerequisite to the study of CP violating asymmetries in B decays, a subject taken up in Section 3. There we lay out the various classes of CP violating asymmetries and re-evaluate the expectations for their magnitude (and hence the number of B mesons needed to establish a statistically significant effect) in the light of the ARGUS measurement.[4] Section 4 takes up the production of t quarks in the now not unlikely case that M_t is comparable to, or larger than M_W. Finally, in Section 5 some of the physics to be explored in t quark decays is considered.

2. The Production of b Quarks at the SSC

The total cross-section for the production of bottom quarks is controlled by the parton processes $gg \rightarrow b\bar{b}$ and $q\bar{q} \rightarrow b\bar{b}$. The former process dominates at SSC energies. In order to calculate the rate we must know; the quark and gluon structure functions at the appropriate values of x and Q^2; the bottom quark mass (m_b); and the partonic cross sections which are presently known only in lowest order,[5] i.e., α_s^2. The values of the momentum fractions x_1 and x_2 of the incoming partons are given by,

$$ x_1 x_2 > \frac{4m_b^2}{s} \quad , \tag{1} $$

where s is the center-of-mass energy squared of the proton-proton system. Since the structure functions are rapidly falling functions of x, the dominant regions of x_1 and x_2 occur where they are equal and of order 2.5×10^{-4}. This raises an immediate problem since the quark distributions are measured only for $x > 0.015$, and the gluon distribution, which must be inferred from the Q^2 dependence of the antiquarks, is known even less well.[6]

A conventional assumption is that $xf(x, Q_0^2)$, for either gluons or sea quarks, tends to a constant as $x \rightarrow 0$. Here Q_0 is some fixed scale at which measurements are made. Such an assumption is not consistent with perturbative QCD. As Q^2 is increased, $xf(x, Q^2)$ takes the following asymptotic form:[7]

$$ x\, f(x, Q^2) \sim \exp \left\{ \sqrt{\tfrac{144}{33-2n_f} \, log\left(\tfrac{1}{x}\right) \, log[log(Q^2)]} \right\} \tag{2} $$

at small x. Here n_f is the number of light quark flavors. Collins[8] has argued that a better form at Q_0^2 is obtained by assuming that $x\, f(x, Q_0^2) \sim x^{-1/2}$, which is more stable with respect to the Q^2 evolution. Figure 1 shows the difference in these two assumptions at $Q_0^2 = 5$ GeV^2. The relevant Q^2 for the total bottom quark rate is of order $4m_b^2$, the minimum value of the center-of-mass energy squared in the parton system. Figure 1 also shows how the two different starting distributions have evolved at $Q^2 = 100$ GeV^2. Notice that the large differences at $Q^2 = 5$ GeV^2 have washed out to some extent. The differences at small x can be probed either at HERA or by measuring Drell–Yan dilepton production at low invariant mass at the Tevatron collider,[9] and should be resolved before the SSC starts running.

The total cross section for bottom pair production is shown in Figure 2, where a bottom quark mass of 4.9 GeV has been assumed. Two curves which are shown reflect the choices in Figure 1 for the distribution functions. It can be seen that the differences are larger at SSC than at the Tevatron since the values of x are smaller. Until we have better data on structure functions we cannot know where the true answer lies. However the upper curve is likely to be nearer the truth than the lower one.
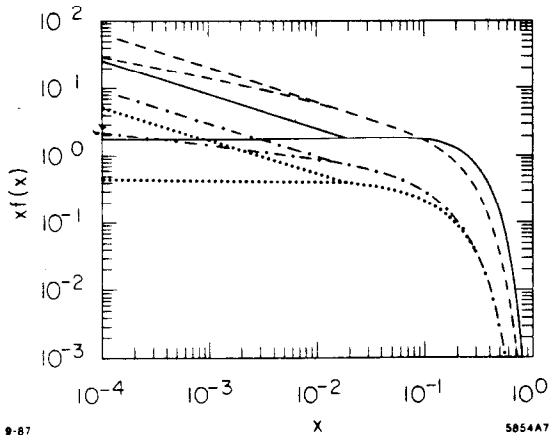
Fig. 1. The x dependence of $xf(x, Q^2)$ for gluons (dashed and solid lines) and antiquarks (dotted and dot-dashed lines) at $Q^2 = 5$ GeV^2 (solid and dotted lines) and $Q^2 = 100$ GeV^2 (dashed and dot-dashed lines). In each case two lines are shown, with the upper one corresponding to the choice $xf(x, 5) \sim x^{-1/2}$ and the lower one to $xf(x, 5) \sim const$ for $x < 0.02$.
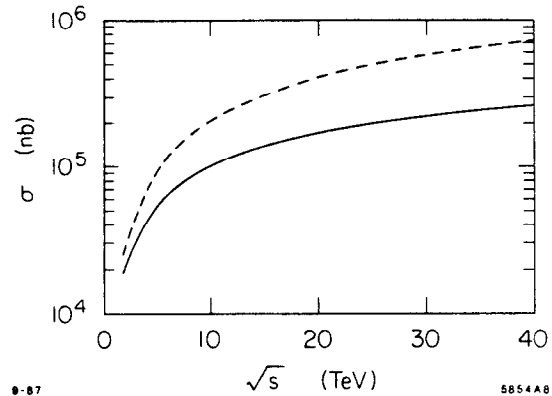

Fig. 2. The total cross section for $pp \to b\bar{b} + X$ as a function of $\sqrt{s}$.

Since the cross section varies roughly as m_b^{-3} over the relevant range, there is an uncertainty of order 50% associated with the choice of a bottom quark mass. The scale Q which appears in α_s (the partonic cross section is proportional to α_s^2) and in the structure functions, is unknown. It should be of order $4m_b^2$, but a better determination is possible only after the order α_s^3 contributions to the partonic cross section have been computed.[10] A bad choice of scale will result in large corrections.

The rapidity distribution of the produced b quarks is flat out to rapidities of ~ 4, as shown in Figure 3. It should be noted that the produced b and $\bar{b}$ are close in rapidity. This is because the rapidity separation is related to the invariant mass, $\sqrt{x_1 x_2 s}$, of the $b\bar{b}$ system, which likes to be small since the parton distributions fall rapidly with x. The transverse momentum distribution is shown in Figure 4. Notice that it is dominated by values of p_T of order m_b. The effect of the uncertainty in the structure functions is much less at large p_T since the relevant values of x are larger.
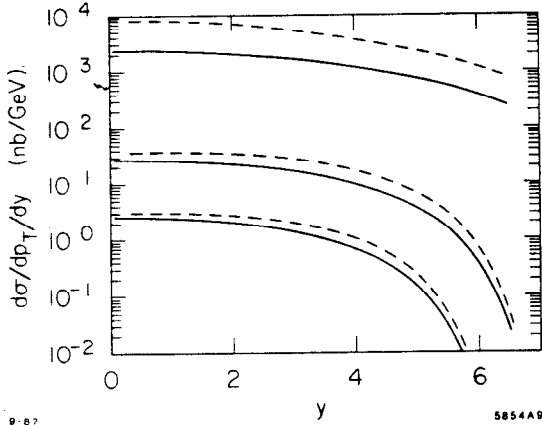
4

Fig. 3. The cross section $d\sigma/dp_T\ dy$ for the production of a b quark in pp collisions at $\sqrt{s} = 40$ TeV as a function of rapidity .y at $p_T = 5$, 30, and 55 GeV. The solid (dashed) line corresponds to the choice $xf(x,5) \sim$ const. $(xf(x,5) \sim x^{-1/2})$. The scale Q^2 appearing in α_s and $f(x,Q^2)$ has been set to $4m_b^2 + p_T^2$.

Fig. 4. The cross section $d\sigma/dp_T\ dy$ for the production of a b quark in pp collisions at $\sqrt{x}=40$ TeV as a function of p_T at $y = 0$. The solid (dashed) line corresponds to the choice $xf(x,5) \sim$ const. $(xf(x,5) \sim x^{-1/2})$. The scale Q^2 appearing in α_s and $f(x,Q^2)$ has been set to $4m_b^2 + p_T^2$.

If one is interested in the production of $b's$ with a transverse momentum much larger than their mass, then other partonic processes can become important. A gluon produced at large transverse momentum can "decay" into a quark antiquark pair.[11] This decay probability can be computed in the leading logarithm approximation, with the result shown in Figure 5. Since the production of a gluon jet at large p_T occurs with a rate which is of order 200 times[12] that for the direct production of a b via $gg \to b\bar{b}$, this mechanism will dominate at large p_T. The rate is much larger than that shown in Figure 4 at very large p_T. Notice that the kinematics of the gluon decay process is quite different from that of $gg \to b\bar{b}$; in the latter case the transverse momentum

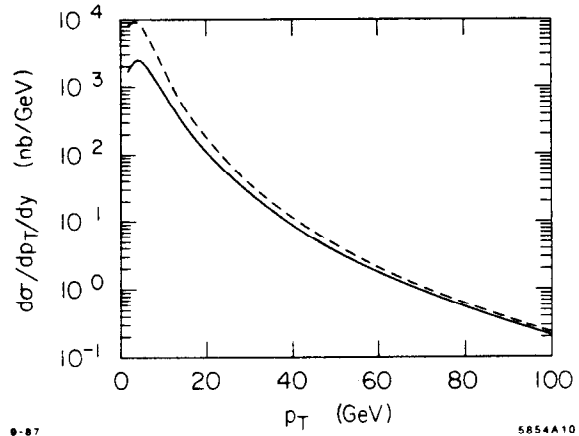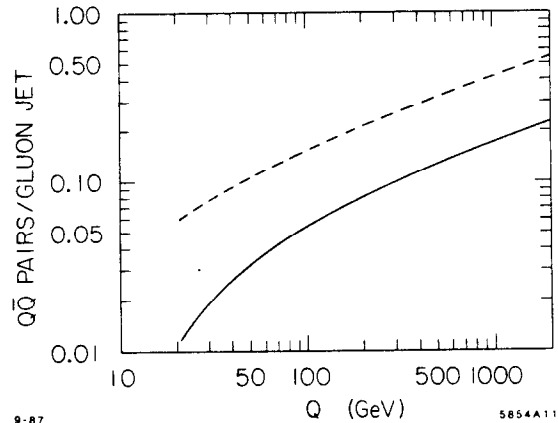Fig. 5. The average number of heavy quark pairs resulting from the fragmentation of a gluon jet as a function of the off-shellness, Q, of the gluon jet. For jets produced in pp collisions, Q is of order p_T. (Solid: $b\bar{b}$, dashed: $c\bar{c}$.)

5

of the b is balanced against that of the $\bar{b}$, whereas in the former case, the b and $\bar{b}$ are on the same side, their transverse momenta being balanced by a gluon jet.

The dominance of this gluon decay process at large p_T does not imply that the total rate calculated from $gg \to b\bar{b}$ is subject to large higher order QCD corrections. Such a conclusion cannot be drawn unless all the order α_s^3 processes are computed. There is also the so-called flavor excitation process where the bottom quark is produced via the scattering of a gluon off a bottom quark, which appears as a constituent of the proton through the QCD evolution of the structure functions. Since this bottom quark has arisen from the splitting process $g \to b\bar{b}$, the full process is $gg \to gb\bar{b}$, which is one of the order α_s^3 processes and should therefore not be included in the absence of a complete calculation.

It is of interest to compare the predictions of cross sections with those measured at current energies. The rates predicted for charm production tend to be too low, unless a very small value (of order 1.1 GeV) is used for the charm quark mass. However, charm is not very heavy and the validity of QCD for such small scales is in doubt. There is a measurement of the $b\bar{b}$ rate in $p\bar{p}$ collisions at 630 GeV by the UA1 collaboration. The value[13] of $1.1 \pm .1 \pm .4$ μb for $p_T > 5$ GeV and $|y| < 2$ is in very good agreement with the expected cross section. There is also a measurement[14] in a pion beam at CERN. Here the theoretical uncertainties are larger since the pion structure function is not well known. Nevertheless, the observed value is in reasonable agreement with expectations.[15]

The Monte-Carlo event generators ISAJET[16] and PYTHIA[17] have the parton processes $gg \to b\bar{b}$ and $q\bar{q} \to b\bar{b}$. They also include the gluon "decay" contribution in the leading log approximation. The structure functions used are of the type $xf(x,5) \sim$ const. at small x, and so they may tend to underestimate the total rate.

3. CP Violation in B Meson Decays

Just as the study of K mesons during more than 30 years has contributed enormously to our present understanding of weak interactions, we believe that B meson decays will very likely be the arena in which to reveal various new weak interaction phenomena in the future. One possibility lies in rare decays—for example, flavor changing neutral currents or lepton number violating processes. Another, less revolutionary possibility, lies within the standard model. With the source of CP violation in this case being a single phase in the Kobayashi–Maskawa matrix, large CP violating asymmetries of ~ 10 to $\sim 30\%$ are predicted in certain decays of B mesons.

Thus, if we can attain the requisite sensitivity, we are faced with a situation in which, at the very least, we verify the dramatic predictions of the standard model. At the most, we could discover more interesting phenomena which point beyond the standard model. With an integrated luminosity of 10^{40} cm^{-2}, several times 10^{12} $b\bar{b}$ pairs are produced at the SSC, so that even with reduced luminosity or a moderate acceptance the 'raw' data rate to attempt this kind of experiment is there. The study of B physics at SSC is guaranteed to be very interesting.

Mixing and CP Violation

Mixing describes a situation where the mass eigenstates are a coherent superposition of a particle and antiparticle.[18,19] The time evolution of a meson that was produced as a $B^\circ(\bar{b}d)$ or $\bar{B}^\circ(b\bar{d})$ meson at time t = 0 is given by

$$|B^\circ(t)> = g_+(t)|B^\circ> + \frac{q}{p}g_-(t)|\bar{B}^\circ>$$

$$|\bar{B}^\circ(t)> = \frac{p}{q}g_-(t)|B^\circ> + g_+(t)|\bar{B}^\circ> \quad ,$$

(3)

where

$$g_\pm(t) = \exp\{-\frac{1}{2}\Gamma_1 t\} \exp\{im_1 t\}\left(1 \pm \exp\{-\frac{1}{2}\Delta\Gamma t\} \exp\{i\Delta m t\}\right)/2$$

and we have made the definitions:

$$\Delta\Gamma = \Gamma_2 - \Gamma_1; \quad \Delta m = m_2 - m_1; \quad \frac{q}{p} = \frac{1-\epsilon_B}{1+\epsilon_B} \quad .$$

(4)

Γ_i and m_i, $i = 1,2$ are the width and mass, respectively, of the two mass eigenstates B_i. In the following we set $\Delta\Gamma = 0$ for convenience; for B° mesons, one computes $\Delta\Gamma << \Gamma$ with considerable confidence, as we see below.

Using B mesons one can study rare decays, mixing, and CP violation, all of which will critically test the standard model, aside from the possibility of surprises which will point to new physics. Below we shall concentrate on CP violation and give short explanations for six classes of CP asymmetries in B decays which are relevant for SSC physics.

- Class I—The Charge Asymmetry in Same Sign Dileptons

The charge asymmetry in $B^\circ\bar{B}^\circ \to \ell^\pm\ell^\pm + X$ is given by[20]

$$\frac{\sigma(B^\circ\bar{B}^\circ \to \ell^+\ell^+ + X) - \sigma(B^\circ\bar{B}^\circ \to \ell^-\ell^- + X)}{\sigma(B^\circ\bar{B}^\circ \to \ell^+\ell^+ + X) + \sigma(B^\circ\bar{B}^\circ \to \ell^-\ell^- + X)} = \frac{|\frac{p}{q}|^2 - |\frac{q}{p}|^2}{|\frac{p}{q}|^2 + |\frac{q}{p}|^2}$$

$$= \frac{\text{Im}(\Gamma_{12}/M_{12})}{1 + \frac{1}{4}|\Gamma_{12}/M_{12}|^2}$$

(5)

where we define $< B^\circ |H| \bar{B}^\circ >= M_{12} + \frac{i}{2}\Gamma_{12}$. In order to estimate the size of this asymmetry consider

$$\left|\frac{\Gamma_{12}}{M_{12}}\right| = \left|\frac{\Gamma_{12}}{\Gamma}\right| \left|\frac{\Gamma}{M_{12}}\right| = \frac{2}{x}\left|\frac{\Gamma_{12}}{\Gamma}\right| \quad , \tag{6}$$

where we used the definition

$$x = \frac{\Delta m}{\Gamma} = \frac{2|M_{12}|}{\Gamma} \quad .$$

Now, to estimate Γ_{12}, note that it gets contributions from B° decay channels which are common to both B° and $\bar{B}^\circ$. For example, one may consider a Cabibbo-suppressed decay channel $B \to D\bar{D} + \text{pions} \to \bar{B}$. If this is the only relevant process one might guess

$$\left|\frac{\Gamma_{12}}{\Gamma}\right| \sim 10^{-3} \quad . \tag{7}$$

Putting these numbers into Eq. (6) with $x = 0.78$, the central value of ARGUS,[4] we obtain

$$\left|\frac{\Gamma_{12}}{M_{12}}\right| \sim 2 \times 10^{-3} \quad . \tag{8}$$

Inevitably there are other decay channels which contribute, and there generally will be cancellations among those channels. Nevertheless, in the standard model the CP asymmetry in Eq. (5) should not exceed 10^{-2}, but at the other extreme, we can not be sure it is less than 10^{-3}.

- Class II—Mixing With Decay to a CP Eigenstate

Since there is substantial $B^\circ - \bar{B}^\circ$ mixing, one can consider two decay chains:

$$\begin{matrix} B^\circ \to B^\circ \searrow \\ & f \quad , \\ B^\circ \to \bar{B}^\circ \nearrow \end{matrix}$$

where f is a CP eigenstate. The amplitudes for these decay chains can interfere and generate nonzero asymmetries between $\Gamma(B^\circ(t) \to f)$ and $\Gamma(\bar{B}^\circ(t) \to f)$.

An analysis using Eq. (3), which parallels that for the K meson system, gives

$$\Gamma(B^0(t) \to f) \sim e^{-\Gamma t}\Big\{\Big(1 + \cos[\Delta m\ t]\Big)|\rho|^2$$
$$+ \Big(1 - \cos[\Delta m\ t]\Big)|\frac{q}{p}|^2 + 2\sin[\Delta m\ t]\ \mathrm{Im}(\frac{q}{p}\rho^*)\Big\} \tag{9a}$$

$$\Gamma(\bar{B}^\circ(t) \to f) \sim e^{-\Gamma t}\Big\{\Big(1 + \cos[\Delta m\ t]\Big)$$
$$+ \Big(1 - \cos[\Delta m\ t]\Big)|\frac{p}{q}\rho|^2 + 2\sin[\Delta m\ t]\ \mathrm{Im}(\frac{p}{q}\rho)\Big\} \tag{9b}$$

Here $\rho = A(B \to f)/A(\bar{B} \to f)$. Noting that $|\frac{p}{q}| \sim 1 + \frac{1}{2}\mathrm{Im}\frac{\Gamma_{12}}{M_{12}}$ and $|\mathrm{Im}\frac{\Gamma_{12}}{M_{12}}| \ll 1$, we can set $|\frac{p}{q}| = 1$ to a very good approximation. Using CPT to set $|\rho| = 1$, Eq. (9) simplifies to:

$$\Gamma(\bar{B}^\circ(t) \text{ or } B^\circ(t) \to f) \sim e^{-\Gamma t}\Big\{1 \pm \sin[\Delta m\ t]\mathrm{Im}(\frac{p}{q}\rho)\Big\}\quad, \tag{10}$$

The study of CP violation in these modes requires information on the identity of the B, i.e., whether it is a B° or $\bar{B}^\circ$ at $t = 0$. Since b and $\bar{b}$ quarks are pair produced at SSC, such information can be obtained by tagging the other particle as to its b or $\bar{b}$ content. The observable asymmetry in the case where a B^+ or B^- is used as the "tag" is

$$\frac{\Gamma(\bar{B}^\circ(t) \to f) - \Gamma(B^\circ(t) \to f)}{\Gamma(B^\circ(t) \to f) + \Gamma(\bar{B}^\circ(t) \to f)} = \sin[\Delta m\ t]\ \mathrm{Im}(\frac{p}{q}\rho). \tag{11}$$

If the "tag" is also a neutral B which can oscillate, the situation is slightly more complicated and oscillation of both B° and $\bar{B}^\circ$ must be taken into account. With a common final state f and a semileptonic tag of the associated neutral B, the decays of a $B\bar{B}$ pair in a coherent state of given charge conjugation are,

$$BR\Big(B(t)\bar{B}(\bar{t})\ |_{C=\mp 1} \to f + (D\ell\bar{\nu}X)_{\mathrm{tag}}\Big)$$
$$\propto e^{-\Gamma(t+\bar{t})}\{1 - \sin[\Delta m\ (t \mp \bar{t})]\ \mathrm{Im}(\frac{p}{q}\rho)\} \tag{12a}$$

$$BR\Big(\bar{B}(t)B(\bar{t})\ |_{C=\mp 1} \to f + (\bar{D}\ell\nu\bar{X})_{\mathrm{tag}}\Big)$$
$$\propto e^{-\Gamma(t+\bar{t})}\{1 + \sin[\Delta m\ (t \mp \bar{t})]\ \mathrm{Im}(\frac{p}{q}\rho)\}\quad. \tag{12b}$$

Note that for $C = -1$, i.e., $B\bar{B}$ in an odd relative angular momentum state, the potential asymmetry vanishes if the times t and $\bar{t}$ are treated symmetrically. For example, when

$C = -1$ Eqs. (12a) and (12b) become identical when $t = \bar{t}$. Furthermore, they become equal when the rates are integrated over time. This tends to reduce the value of the observable asymmetry slightly, but for the present purposes we shall ignore this effect (from production of $B^\circ \bar{B}^\circ$ pairs in a $C = -1$ state). Then the process where one B decays to a CP eigenstate and the other B is tagged gives an observable asymmetry which can be written as

$$\frac{\Gamma(B\bar{B} \to f + \bar{\ell}_{\text{tag}}) - \Gamma(B\bar{B} \to f + \ell_{\text{tag}})}{\Gamma(B\bar{B} \to f + \bar{\ell}_{\text{tag}}) + \Gamma(B\bar{B} \to f + \ell_{\text{tag}})} = \sin[\Delta m\, t]\, \text{Im}(\frac{p}{q}\rho) \quad . \qquad (13)$$

For example, possibilities for the final state f are ψK_s, $\psi K_s X$, $\psi \pi^+ \pi^-$, $D\bar{D}K_s$, $\pi^+\pi^-$, D^+D^-, and $D^{0*}\bar{D}^\circ$ + c. c. . Obviously, the "lepton tag" shown above can be replaced by any decay mode which identifies the particle or antiparticle nature of the associated B.

We stress that *in this class of asymmetries the quantities* $\text{Im}(\frac{p}{q}\rho)$ *can be predicted from the Kobayashi–Maskawa matrix.* The hadron dynamics cancel in the ratio of amplitudes ρ. Since $|\frac{p}{q}| \approx 1$, as described above, and for a CP eigenstate $|\rho| = 1$, we can write

$$\frac{p}{q}\rho_f = e^{i\phi_q} \quad . \qquad (14)$$

For a B_q° meson, it can be shown that the phase on the right-hand-side of Eq. (14) is

$$\phi_q = 2 \arg \left([U_{tb}\, U_{tq}^*] \begin{bmatrix} U_{cb}^*\, U_{cs} \\ U_{cb}^*\, U_{cd} \\ U_{ub}^*\, U_{ud} \end{bmatrix} \right) \quad \text{for} \quad \begin{matrix} b\bar{q} \to c\bar{c}s\bar{q} \\ b\bar{q} \to c\bar{c}d\bar{q} \\ b\bar{q} \to u\bar{u}d\bar{q} \end{matrix} \quad , \qquad (15)$$

giving an explicit formulation in terms of KM matrix elements. In the Wolfenstein parameterization[21] of the KM matrix

$$U_{KM} = \begin{pmatrix} 1 - \lambda^2/2 & \lambda & \lambda^3 A(\rho - i\eta) \\ -\lambda & 1 - \lambda^2/2 & \lambda^2 A \\ \lambda^3 A(1 - \rho - i\eta) & -\lambda^2 A & 1 \end{pmatrix} \quad . \qquad (16)$$

An explicit example is provided by the process $b\bar{d} \to c\bar{c}s\bar{d}$, where substituting the Wolfenstein parametrization into Eq. (15) gives[21]

$$\text{Im}(\frac{p}{q}\rho) = \text{Im}(e^{i\phi_d}) = \frac{2(1 - \rho)\eta}{(1 - \rho)^2 + \eta^2} \quad . \qquad (17)$$

Numerically, $\lambda = \sin\theta_C = .22$, $|U_{cb}| = .045 \pm .008$ implies $A = .93 \pm .17$, and $|U_{ub}/U_{cb}| < .19$ implies $\rho^2 + \eta^2 \lesssim .75$. The value of η is constrained by the measurement of ϵ, expressing

10
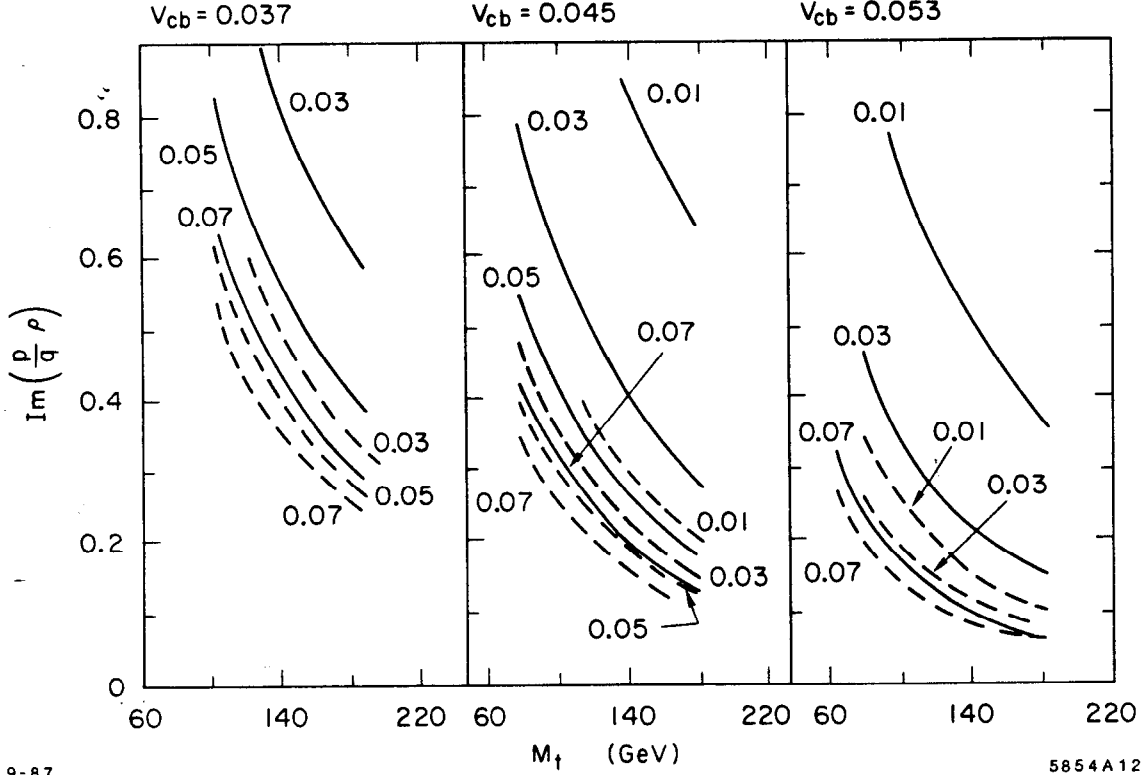
Fig. 6. Values of $\mathrm{Im}\left(\frac{p}{q}\rho\right)$ as a function of the mass of the top quark, M_t, for various values of the Kobayashi–Maskawa matrix element, U_{cb}, with dashed curves corresponding to the process $b\bar{q} \to c\bar{c}s\bar{q}$ and solid curves corresponding to the process $b\bar{q} \to u\bar{u}d\bar{q}$. The parameter B_K is taken to be unity, and the curves are labelled by the ratio of the rates, $\Gamma(b \to u)/\Gamma(b \to c)$.

the strength of CP violation in the K meson system. For given values of U_{cb}, of $\rho^2+\eta^2$, i.e., fixed $\Gamma(b \to u)/\Gamma(b \to c)$, of M_t, and of the parameter B_K, which is equal to unity when the matrix element of the $\triangle S = 2$ operator giving rise to the $K_L - K_S$ mass difference has its vacuum insertion value, the constraint coming from ϵ gives two possible values for ρ and η. For those values of ρ and η, we compute $\triangle m_B$ for the $B_d - \bar{B}_d$ system and choose the solution which gives a larger value of $\triangle m_B$. Finally, for the values of ρ and η which satisfy the above criteria, we compute $\mathrm{Im}(\frac{p}{q}\rho)$, which is shown in Figure 6. The alternative choice of ρ and η, which gives a smaller value of $\triangle m_B$, leads to larger values of $\mathrm{Im}(p/q)\rho$. In what follows we shall take

$$0.1 < \mathrm{Im}\left(\frac{p}{q}\rho_f\right) < 0.6$$

11

- **Class III**

For those final states which are not CP eigenstates, for example,[22]

$$\overset{(-)}{B_d} \to D^- \pi^+ \quad , \quad D^+ \pi^- \ldots$$

$$\overset{(-)}{B_s} \to F^+ K^- \quad , \quad F^- K^+ \ldots \quad ,$$

one can follow a similar analysis and form an asymmetry

$$\frac{\Gamma\left(B\overline{B} \to f + \ell \ldots\right) - \Gamma\left(B\overline{B} \to f^{CP} + \ell \ldots\right)}{\Gamma\left(B\overline{B} \to f + \ell \ldots\right) + \Gamma\left(B\overline{B} \to f^{CP} + \ell \ldots\right)}$$

$$= \frac{2\sin[\triangle m\, t]\, \mathrm{Im}\left(\frac{p}{q}\, \rho\right)}{\left(1 + |\rho|^2\right)} \tag{18}$$

where

$$\rho = \frac{A(B \to f)}{A(\bar{B} \to f)} \quad ,$$

as before, but now ρ depends on hadron dynamics. For example, using a factorization ansatz to compute the hadronic matrix element,

$$\rho_f = \frac{A\left(B_d \to D^+ \pi^-\right)}{A\left(\bar{B}_d \to D^+ \pi^-\right)} \approx \frac{U_{ub}^* U_{cd} f_D m_B^4}{U_{cb} U_{ud}^* f_\pi \left(m_B^2 - m_D^2\right)^2} \tag{19}$$

$$\sim (1 - 2)\lambda^2(\rho + i\eta) \quad ,$$

where our ignorance concerning the correct value for f_D/f_π is the source of the uncertainty in the coefficient of $\lambda^2(\rho + i\eta)$. In addition, there are further uncertainties concerning the validity of the factorization ansatz, etc. In any case, the ratio ρ is not a unit vector in the complex plane, nor then is $\frac{p}{q}\,\rho$ when f is not a CP eigenstate, and in general considerable uncertainties surface. An analogous procedure for B_s decays yields with comparable uncertainties,

$$\rho_f = \frac{A\left(B_s \to F^+ K^-\right)}{A\left(\bar{B}_s \to F^+ K^-\right)} = \frac{U_{ub}^* U_{cs}}{U_{cb} U_{us}^*} \frac{f_F}{f_K} \frac{m_{B_s}^4}{\left(m_{B_s}^2 - m_F^2\right)^2} \tag{20}$$

$$\sim 1.6\left(\rho + i\eta\right) \quad .$$

• Class IV

The two cascade decays shown in Figure 7 lead to the same final states

$$B^- \rightarrow D^\circ s\bar{u}$$

$$\downarrow\!\!\rightarrow K_s^\circ u\bar{u}$$

$$B^- \rightarrow \bar{D}^\circ s\bar{u}$$

$$\downarrow\!\!\rightarrow K_s^\circ u\bar{u}$$

and therefore their amplitudes can interfere. From the quark diagrams in Figure 7, one reads off the Kobayashi–Maskawa matrix element factors which are the coefficients of the two amplitudes,
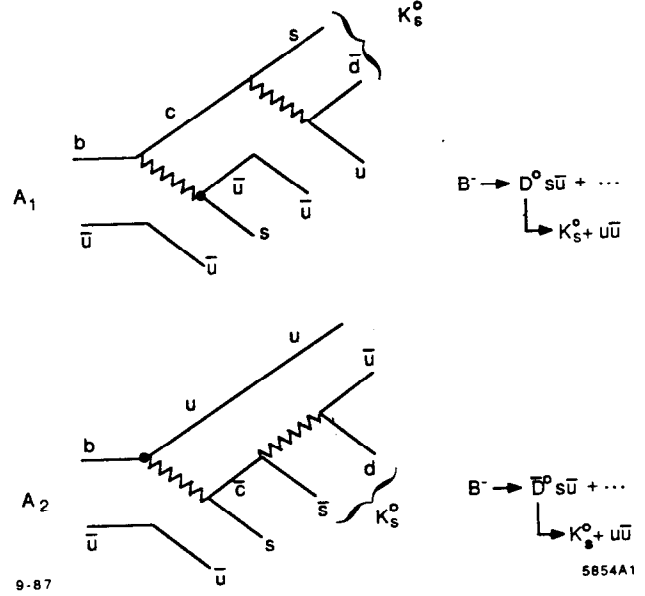

Fig. 7. B_u decay diagrams whose interference can lead to a Class IV asymmetry.

$$A\left(B^- \rightarrow K_s^\circ u\bar{u}s\bar{u}\right) \propto U_{cs}^* U_{cb} U_{us}^* U_{ud} \, A_1 + U_{ub} U_{cs}^* U_{cs} U_{ud}^* \, A_2 \quad . \tag{21}$$

Then the asymmetry can be obtained from

$$\Gamma\left(B^\pm \rightarrow (K_s + X)_D + Y\right) \propto \Bigg\{ 1 + \frac{|U_{ub}|^2 |U_{cs}|^2}{|U_{cb}|^2 |U_{us}|^2} |\bar{\rho}|^2$$

$$+ 2Re\left(\frac{U_{ub} U_{cs} U_{ud}^*}{U_{cb} U_{us} U_{ud}}\right) Re\bar{\rho} \pm Im\left(\frac{U_{ub} U_{cs} U_{ud}^*}{U_{cb} U_{us} U_{ud}}\right) Im\bar{\rho} \Bigg\} \tag{22}$$

where $\bar{\rho} = A_2/A_1$. $Im\bar{\rho}$ where $\bar{\rho} = A_2/A_1$. $Im\bar{\rho}$ comes from the phase shift difference between scattering of $D + (s\bar{u})$ states and $\bar{D} + (s\bar{u})$ states. Since the isospin structures of these states are different, we expect nonvanishing values of $Im\bar{\rho}$. Again, at least compared with a Class II type of asymmetry, the theoretical prediction is quite uncertain.

• Class V

B decays can also receive contributions from quark decay and from weak annihilation diagrams,[23] as shown in Figure 8. They can contribute coherently to modes such as

13

$$B_u \to D^{\circ *} D^- \quad . \tag{23}$$

It is very difficult to estimate the asymmetry for this process. The effect of weak annihilation as well as $c\bar{c}$ pair production must be included in an estimate. An optimistic guess is

$$\frac{\Gamma\left(B^- \to D^{\circ *} D^-\right) - \Gamma\left(B^+ \to \bar{D}^{\circ *} D^+\right)}{\Gamma\left(B^- \to D^{\circ *} D^-\right) + \Gamma\left(B^+ \to \bar{D}^{\circ *} D^+\right)} \sim 10\% \quad . \tag{24}$$
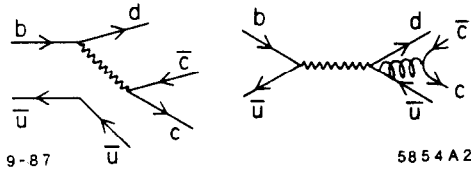

Fig. 8. B_u spectator and annihilation diagrams whose interference can lead to a Class V asymmetry. The spectator diagram is shown in a Fierz transformed manner to indicate more directly the identity of the final state quarks with those from the annihilation diagram.

Fig. 9. B_u penguin and spectator decay diagrams whose interference can lead to a Class VI asymmetry.

- Class VI

Allowing for penguin operators, as shown in Figure 9, opens up another possibility for generating a CP violating asymmetry.[24] A particular channel of interest is

$$B_u^- \to K^- \rho^\circ \quad ,$$

since the signature is rather clear.

A rough estimate gives

$$\frac{\Gamma\left(B^- \to K^- \rho^\circ\right) - \Gamma\left(B^+ \to K^+ \rho^\circ\right)}{\Gamma\left(B^- \to K^- \rho^\circ\right) + \Gamma\left(B^+ \to K^+ \rho^\circ\right)} \sim 10\% \quad . \tag{25}$$

Again, the estimate contains uncertainties, including those due to long distance effects which supply strong interaction phases. Note that we can not only have differences in overall rates, but CP violating asymmetries in the differential rates, *i.e.*, in the Dalitz plot, for certain modes.[25]
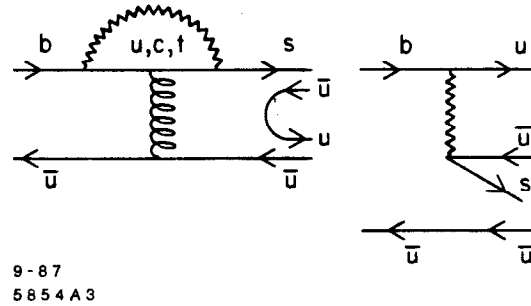
We summarize this subsection by emphasizing again the fact that Class II asymmetries are predicted unambiguously in the KM model and are cleaner theoretically. But it is still very important to search for the other classes of asymmetries. They may be large, and some of them do not require tagging, possibly making them easier to observe experimentally. For example, although we may have eliminated the superweak model by the time SSC experiments begin, a single unambiguous observation of an asymmetry in charged B decays will immediately rule out the superweak model of CP violation, since in that case no asymmetry is expected in decays which do not involve mixing.

Time Dependence

The observation of the secondary vertex for B decay is very likely crucial in isolating events in which B's are produced.[26] This inevitably leads to a loss of events for those B's which decay too early to allow distinguishing the secondary from the primary vertex.

This is balanced by ways in which the time-dependent asymmetry can be used to our advantage. Consider

$$\Gamma\left(\overset{(-)}{B} \to f\right) \propto e^{-T}\left(1 \pm \sin[xT]\,\mathrm{Im}(\frac{p}{q}\,\rho)\right) \quad , \tag{26}$$

where $T = \Gamma t$, is the time in the units of lifetime. Comparing this with the time-integrated expression

$$\Gamma\left(\overset{(-)}{B} \to f\right) \propto \left(1 \pm \frac{x}{1+x^2}\,\mathrm{Im}(\frac{p}{q}\rho)\right) \quad , \tag{27}$$

it is quite clear that for B_s system in which

$$x_s > 6\, x_d \sim 5 \quad , \tag{28}$$

the oscillations tend to wash out the time-integrated asymmetry. Thus an asymmetry measurement for B_s decays must be accompanied by measurement of the secondary vertex with a spatial resolution in the transverse plane of approximately,

$$\ell = \frac{\pi}{10} \cdot \frac{1}{x_s} \cdot \left(100 \mu m\right) \quad .$$

The time dependence of Eq. (26) for $\mathrm{Im}\,((p/q)\rho) = .1$ and $.6$, the conservative and optimistic values, is shown in Figure 10 for the B_d system with $x = 0.78$. Note that the asymmetry vanishes at $T = 0$. Thus by cutting out the events with small values of T, the asymmetry will increase, even though the number of events has decreased.
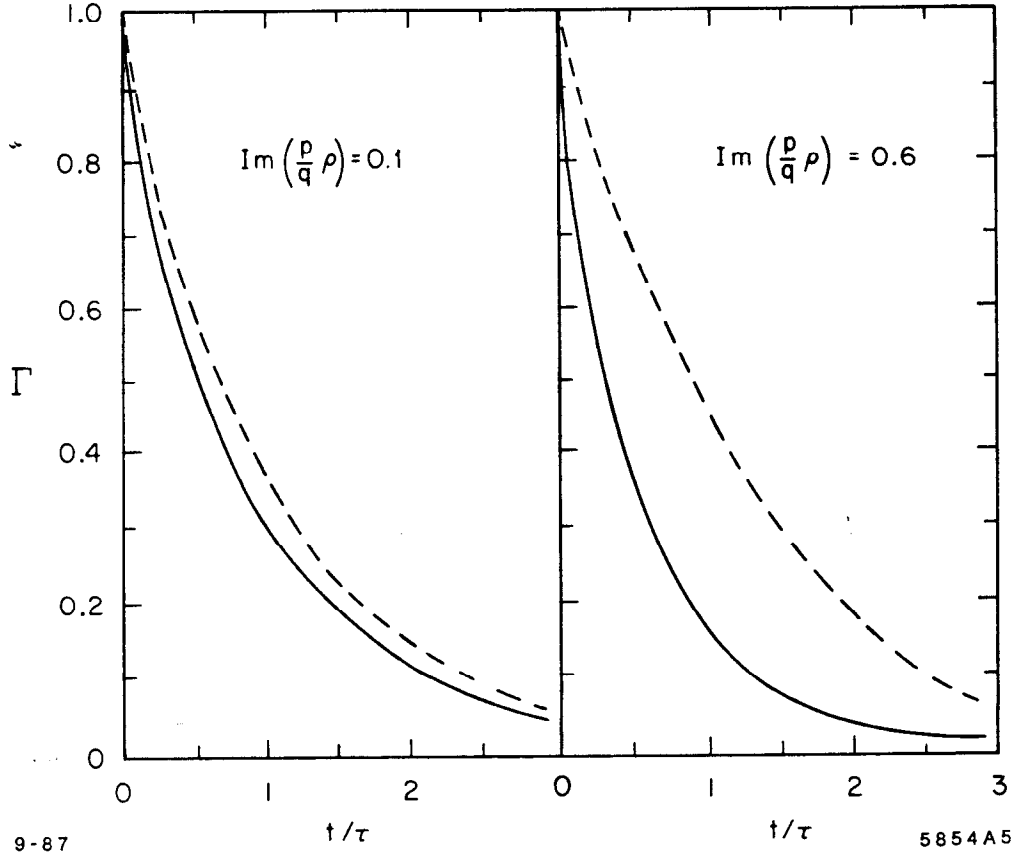
Fig. 10. The time dependence for the decay of a B_d or $\overline{B}_d$ meson to a CP eigenstate, as in Eq. (26), with $x_d = 0.78$, and $\text{Im}\left(\frac{p}{q}\rho\right) = 0.1$ and 0.6.

A crude use of the full information contained in the time dependence is obtained by considering the asymmetry for decays [see Eqs. (9a) and (9b)] occurring between times T_1 and T_2 is given by

$$\text{Asymmetry} = \left\{ \left(e^{-T_1} \cos xT_1 - e^{-T_2} \cos xT_2 \right) x \right.$$

$$\left. + \left(e^{-T_1} \sin xT_1 - e^{-T_2} \sin xT_2 \right) \right\} \frac{\text{Im}(\frac{p}{q}\rho)}{(1 + x^2)(e^{-T_1} - e^{-T_2})} \quad . \tag{29}$$

For example, Figure 11 shows the net asymmetry as a function of T_1 when we set $xT_2 = \pi$. Note that the asymmetry indeed peaks at $T_1 = 1$. A best choice for T_1 can be extracted from the following:

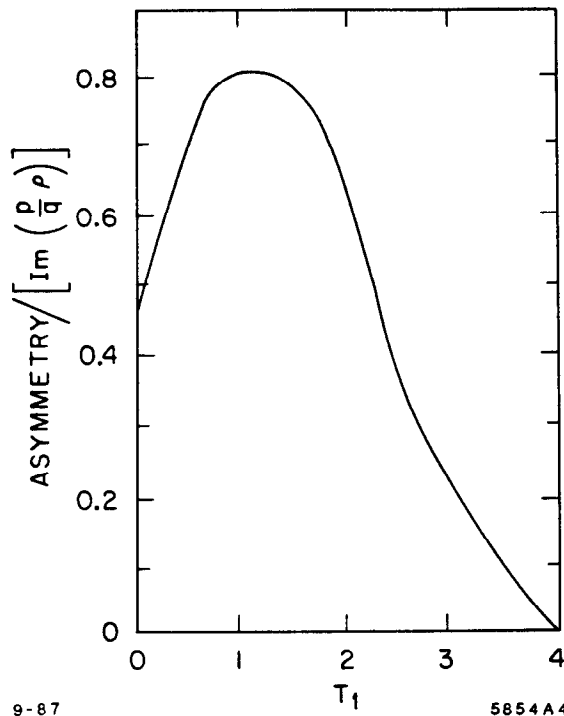| T_1	0	.25	.5	.75	1
$\frac{\text{Asym}(T_1)}{\text{Asym}(O)} e^{-T_1}$	1	1.21	1.29	1.24	1.02

16

Fig. 11. The net asymmetry as a function of the lower cutoff in proper time (in units of the lifetime), T_1, with the upper cutoff set at $T_2 = \pi/x$.

Compared to a case in which there is no t cut ($T_1 = 0$), selecting $T_1 = 1$ reduces the number of available events, but almost exactly compensates for this by a larger asymmetry; such a cut will lead to a measurement with the same statistical significance. Similarly, a cut at $T_1 = 0.5$ will actually give a 30% reduction in the number of events required to obtain an asymmetry of a given significance when compared to an experiment without the T_1 cut.

<div align="center">

**Estimation of the Number of $B\bar{B}$ Events
Required for CP Violation Studies at the SSC**

</div>

Now we proceed to use the theoretical predictions for the CP violation asymmetries in B meson decays developed above to estimate the minimum number of B mesons which would be needed for observing CP violation in an experiment at the SSC. These predictions are divided into the six classes of asymmetries which we have discussed and are summarized in Table I. The estimated number of produced $B\bar{B}$ pairs necessary to yield a three standard deviation effect of a certain class, given a branching ratio, asymmetry, and tagging efficiency (explained below) are given in the last column.

The Table was constructed using input and assumptions as follows:

- The branching ratios given in the third column are in many cases below the level of sensitivity of experiments at the existing e^+e^- machines. For these unmeasured modes, the branching ratios given are purely theoretical estimates.

17

Table 1. Estimation of the number of $B\bar{B}$ events required for CP violation studies at the SSC[*]

Class	Modes	Branching Ratio	Asymmetry	# $B\bar{B}$ Events Required
I. Charge Asymmetry in Same Sign Dileptons	$B_d\bar{B}_d \to \ell^\pm \ell^\pm + X$	0.01	10^{-3}	6×10^9
	$B_s\bar{B}_s \to \ell^\pm \ell^\pm + X$	0.02	10^{-4}	2×10^{12}
II. Mixing with Decay to a CP Eigenstate	$B \to \psi K_s$	5×10^{-4}	$0.05 - 0.3$	$(1 - 34) \times 10^8$
	$B \to \psi K_s X$	2×10^{-3}	$0.05 - 0.3$	$(2 - 85) \times 10^7$
	$B \to D\bar{D}K_s$	5×10^{-3}	$0.05 - 0.3$	$(3 - 100) \times 10^7$
	$B \to \pi^+\pi^-$	5×10^{-5}	$0.05 - 0.5$	$(0.3 - 32) \times 10^8$
	$B \to D^{+*}D^-, D^+D^-, D^*D^*$	3×10^{-3}	$0.05 - 0.3$	$(0.7 - 26) \times 10^8$
III. Mixing with Decay to a CP Non–Eigenstate	$B_d \to D^+\pi^-$	6×10^{-3}	0.001	3×10^{11}
	$B_d \to D^\circ K_s$	6×10^{-5}	0.01	7×10^{11}
	$B_s \to D_s^+ K^-$	3×10^{-4}	0.5 ?	5×10^7
IV. Cascade Decays to the Same Final State	$B^- \to D^\circ K^- + X$ $\quad \hookrightarrow K_s + Y$	10^{-5}	0.1 ?	9×10^8
V. Interference of Spectator and Annihilation Graphs	$B^- \to D^{0*}\bar{D}^-$	3×10^{-3}	0.01	2×10^9
VI. Interference of Spectator and Penguin Graphs	$B^- \to K^-\rho^\circ$	$\sim 10^{-5}$	0.1	1×10^8
	$\bar{B}_d \to K^-\pi^+$	$\sim 10^{-5}$	0.1	1×10^8

[*]The specific channels considered here for each class of asymmetry are illustrative and not exhaustive. At this time we need to keep an open mind as to which channels will be best suited for CP violation studies. In this spirit we have included among the modes illustrating Class II asymmetries $\psi K_s X$ and $D\bar{D}K_s$, which are not necessarily CP eigenstates. There is some danger of a cancellation between the asymmetries produced by sub-channels with opposite CP quantum numbers, but a total cancellation is unlikely.

- The asymmetries were estimated as described above in the discussion of each of the six classes of CP violating asymmetry.

- To observe an asymmetry, a = $(N(B) - N(\bar{B}))/(N(B)+N(\bar{B}))$ with S standard deviation confidence requires a minimum of $(S/a)^2$ B mesons. The number of $B\bar{B}$ events required is calculated from:

$$N(B\bar{B}) = \left(\frac{1}{2}\right)\left(\frac{S^2}{a^2}\right)\left(\frac{1}{\epsilon_{tag} \cdot BR(B \to f) \cdot BR(f \to X_{ch}) \cdot f(B)}\right) \quad , \qquad (30)$$

where ϵ_{tag} is the tagging efficiency (if it is necessary to tag the initial identity of the B or $\bar{B}$), $BR(B \to f)$ is the branching ratio for the CP violating decay mode $B \to f$, $BR(f \to X_{ch})$ is the branching fraction for f decays into stable charged particles, and $f(B)$ is the fraction of B mesons in a jet of the type needed for a given asymmetry measurement. In the Table we use $S = 3$.

- Class I modes require B° - $\bar{B}^\circ$ mixing as well as the detection of both B mesons in their semileptonic decays. The branching ratios in Table 1 account for the semileptonic decay branching ratio of both B mesons (0.04) and the probability that one of the B° mesons mixes and decays to a "wrong" sign lepton. The mesons are then already "tagged" by the charges of the leptons and no other charged particles need be detected.

- When tagging is necessary (in Classes II and III), we propose using the semileptonic decay $B \to D + \ell + X$, where ℓ is an electron or a muon, as the tagging signature for the "other B". Provided that a common vertex is reconstructed for the D and the lepton, the sign of the lepton, aside from mixing, gives the identity of the initial b quark. The presence of a D meson in a common vertex with the lepton provides a powerful discrimination against leptons from semileptonic decays of charm hadrons not originating from B meson decays. The tagging efficiency is the product of the branching ratios for $B \to D + \ell + X$ (~ 0.2), for D decay into all charged final states (~ 0.2), and for a B_d or B_u in the jet (0.76, see below), which combine to make $\epsilon_{tag} \sim 0.03$.

- B meson decays that can produce asymmetries in Classes IV, V, or VI are "self-tagging", i.e., do not require tagging the accompanying B meson. We take their tagging efficiency to be unity.

- Considering the complicated nature of SSC events in the forward region, we assumed that only charged stable particles will be used for reconstructing B meson decays. For the purpose of these calculations, we assumed J/ψ detection in the e^+e^- and $\mu^+\mu^-$ modes, D and D_s detection in all charged particle modes, and K_s detection in $\pi^+\pi^-$ with branching ratios of 0.14, 0.2, 0.1 and 0.67, respectively.

- For the relative population of the various species of B hadrons in a b quark jet we use the fractions $f(B_d^\circ) = 0.38$, $f(B^+) = 0.38$, $f(B_s) = 0.15$ and $f(bqq) = 0.09$.

- The estimated numbers of $B\bar{B}$ events required for observing both the lower and the upper range of the predicted asymmetry in each mode are given in the last column of Table 1. A preliminary study shows that using the full proper life-time dependence of the asymmetry reduces the number of required B_d's by a factor of 1.3 compared to the numbers given in the table for the time-integrated asymmetries. For the B_s meson, where due to maximal mixing many oscillations can occur in one lifetime, we use the full time-dependence information to estimate the required number of events.

These estimates do not include the effect of detection efficiencies. Furthermore, since we have not accounted for background effects, they should only be considered as the minimum number of $B\bar{B}$ events required for CP violation studies at the SSC. Clearly, a realistic assessment of such an experiment requires a detailed study of the background effects as well as of detection efficiencies, including effects due to geometrical acceptance, tracking, momentum and energy resolution, vertex reconstruction, particle identification, and triggering efficiency.

4. The Production of t Quarks at the SSC

Recent limits[27] from UA1, indicating that the mass of the top quark is larger than 44 GeV, together with theoretical interpretation[28] of the ARGUS result[4] on $B - \bar{B}$ mixing have increased considerably the possibility that M_t is comparable to, or even greater than, M_W. The production and detection of the t quark when $M_t < M_W$ has been considered previously.[29,30] Now the question of the production and signatures of top quarks with $M_t > M_W$ at the SSC needs to be examined, together with the resulting lepton spectra from cascade decays of the top quark.[31] Heavy top quark production is interesting in another way in that it turns out to be a severe background in the search for a heavy Higgs boson in the W^+W^- decay mode.[31]

The results have been obtained with the ISAJET Monte Carlo[16] and concentrate on the measurement of muons from t quark decays, assuming a high resolution muon detector, like L3+1. The momentum resolution is taken to be $\delta p/p = 4 \times 10^{-5}\, p$, with p in GeV/c. An angular coverage of $5° < \theta < 175°$ is assumed, and only muons with $p_T > 10$ GeV have been used for the analysis.

Top quarks with $M_t > M_W$ are mainly produced through gluon-gluon fusion. Figure 12 shows the total cross section for $t\bar{t}$ production as a function of the t mass for $p_T > 10$ GeV and $p_T > 100$ GeV. The cross sections have an uncertainty of about a factor 2, because of poor knowledge of the gluon density function at very small values of x. For $\int L dt = 10^{40}\, cm^{-2}$ at $\sqrt{s} = 40$ TeV one expects 1.8×10^8 events (2.6×10^7) for $M_t = 100$ GeV (200 GeV) and $p_T^{top} > 100$ GeV. At $p_T > 100$ GeV the cross section for b quark production is 3 (21) times larger than for a top quark with mass $M_t = 100$ GeV (200 GeV).

Since the t quark decays into a W boson and a b quark, the final state in $gg \rightarrow t\bar{t} \rightarrow W^+ W^- b\bar{b}$ consists of two W bosons and two b jets. For $M_t = 100$ GeV, the mean
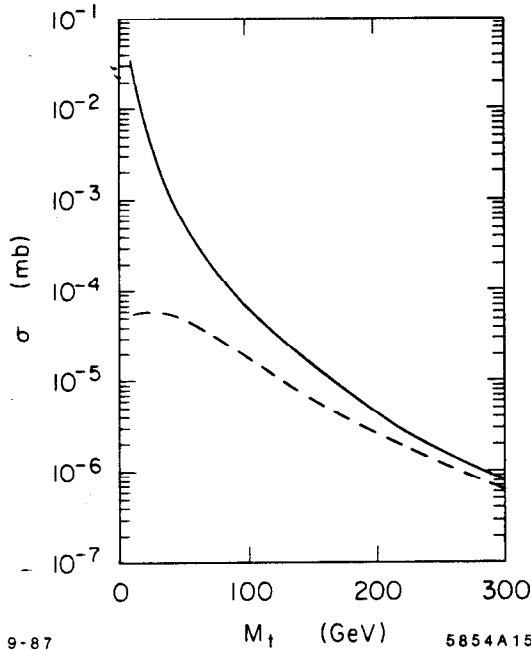
transverse momentum of the b jet is about 20 GeV. The p_T of the b jets is especially small if the mass of the top quark is only slightly larger than M_W. The decay of a heavy top quark represents a large source of W pairs at the SSC, being about two orders of magnitude larger than the continuum production.

A relatively clean signal for heavy t quark production is obtained if one W boson decays leptonically (into a muon plus a neutrino) and the other hadronically (into quarks). One then observes an isolated muon and a low p_T b jet, balanced on the other side by 2 jets from the W decay and a low p_T b jet. To further reduce QCD background from high p_T W production, one can study events with two muons produced in the cascade decay of the top quark:

$$t \rightarrow W^+ + b \rightarrow \mu^+\nu_\mu + \mu^-\bar\nu_\mu + c \quad .$$

Fig. 12. The cross section for $t\bar{t}$ production in pp collisions at $\sqrt{s} = 40$ TeV as a function of the mass of the top quark, M_t, and $p_T > 10$ GeV (solid curve) and $p_T > 100$ GeV (dashed curve).

The background from high p_T $b\bar{b}$ and $c\bar{c}$ production can be reduced by requiring that the

high p_T muon be isolated. If one requires the energy in the calorimeter to be less than 10 GeV inside a cone of $\Delta R < 0.3$ around the high p_T muon, one can reduce the light quark background to a sufficiently low level. We are taking advantage of the signature of heavy top decay being an isolated high p_T muon plus a second low p_T muon inside the bottom quark jet. The mean p_T of both muons has a strong dependence on the top mass, with the ratio of the mean transverse momenta of the muons, $< p_T(\mu_W) > / < p_T(\mu_b) >$ being about 10 for $M_t = 100$ GeV. This ratio can be used to measure M_t.
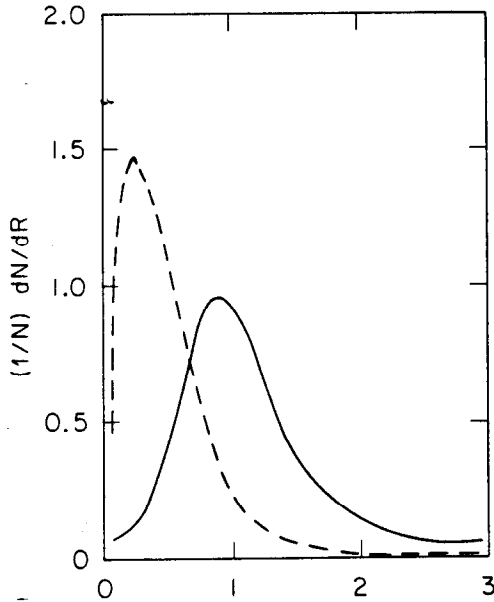
Another method to determine the t quark mass is through the distribution of $R = \sqrt{(\Delta\eta)^2 + (\Delta\phi)^2}$, which measures the separation in space between the muons from the W and b decay ($\Delta\phi$ is the difference in azimuthal angle of the muons with respect to the proton beam, and $\Delta\eta$ the difference in their pseudo-rapidities.) This is shown in Figure 13 for $p_T = 300$ GeV. The distributions are clearly distinct for $M_t = 100$ GeV and 200 GeV. Thus a measurement of R at fixed p_T^{top} is a measure of the mass of the t quark, where p_T^{top} is measured from the total p_T of the jets opposite to the muon pair.

Fig. 13. The distribution in R between the muons coming from W and b decay for $M_t = 100$ (dashed curve) and $M_t = 200$ GeV (solid curve) and $p_T^{top} = 300$ GeV.
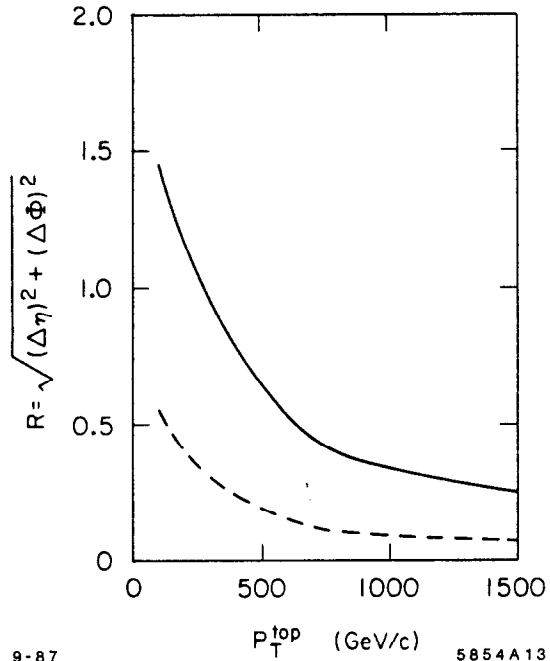
Fig. 14. The average value of R as a function of the transverse momentum of the top quark, p_T^{top}, for values of $M_t = 100$ (dashed curve) and $M_t = 200$ (solid curve) GeV.

Figure 14 shows the average R as function of the p_T of the primary t quark. This measurement can provide a fairly precise determination of the mass of the t quark. The event rate at the SSC is sufficiently high to allow for this measurement. Even for $p_T^{top} > 1$ TeV, from the gluon-gluon fusion production mechanism alone one still expects 1800 events with lepton pairs from the cascade decay of the t quark when the integrated luminosity, $\int L dt = 10^{40} cm^{-2}$.

5. The Physics of t Quark Decays

If we limit our scope to three generations of quarks and leptons, then a great deal of the physics of t decays is fixed. The t mass is constrained to be above 25 GeV from TRISTAN,[32] above 44 GeV from UA1,[27] and above about 50 GeV from considerations of $B - \bar{B}$ mixing.[28] That means that M_b/M_t is certainly < 0.2, and is quite likely < 0.1. These are small numbers, smaller than the ratio of final to initial quark masses in the dominant charm or bottom decays, and small enough to be negligible to the accuracy

necessary for most considerations (but see below for a special situation). For example, standard formulas then tell us that 99.7% of t decays will be of the form:

$$t \rightarrow b + W^+ \quad ,$$

with the W^+ being either real or virtual, depending on the t mass. Since $|U_{ts}| \approx |U_{cb}|$ when the KM angles are small (as they are known to be), and $|U_{cb}|$ is known from the B lifetime, we may already say that

$$t \rightarrow s + W^+$$

will only be a $\approx 0.2\%$ decay mode. It is convenient to break the discussion up into the cases where the t quark is lighter or heavier than the W.

- $M_t < M_W$.

    The t decays into a b plus a virtual W, which materializes as $e^+\nu_e, \mu^+\nu_\mu, \tau^+\nu_\tau$, $u\bar{d}$, and $c\bar{s}$, so that in the standard formula

$$\Gamma(t \rightarrow \text{all}) = N \; \Gamma(t \rightarrow q_{-1/3} \; e^+ \; \nu_e) = N \frac{G_F^2 M_t^5}{192\pi^3} \quad , \tag{31}$$

N, the total number of lepton flavors and quark flavors and colors, is equal to 9. This means a total width of ≈ 70 keV for $M_t = 50$ GeV, a number that needs to be corrected slightly upward for QCD, slightly downward for the final quark masses (in particular, the b quark mass, which has been neglected), and upward for the effects of the finite W mass. This latter is the biggest effect, and amounts to $\approx 25\%$ for the case ($M_t = 50$ GeV) cited above.[33] This corresponds to far too short a lifetime to allow separation of a production from a decay vertex, but also far too small a width to be within conceivable experimental resolution. The rate for weak decay of the constituent t quarks within possible hadrons is now comparable with that for electromagnetic and strong decays. Weak decays of toponium become a major fraction of, say, the $J^P = 1^-$ ground state, and even for the $T^*(t\bar{q})$ meson, weak decays can dominate the radiative magnetic dipole transition from this 1^- state to the 0^- ground state.[34]

A t quark in this mass range will very likely be discovered and its properties examined in detail well before the SSC is operating. Depending on its precise mass, TRISTAN, SLC, TEV I, LEP I, and LEP II all have a shot at the initial discovery. A detailed exploration of the properties of the t in its weak decays is the property of the e^+e^- machines. It should be possible, by finding the ground state of toponium to determine M_t to ±0.2 GeV, or better.[35] In principle, the $V - A$ nature of the $t \rightarrow b$ transition can be checked by using longitudinally polarized electrons to form a polarized 1^- toponium state, and then examining the correlation of the momentum of the final lepton with the spin direction of the t quark when it decays semileptonically. Moreover, the fact that t quark weak decays

are competitive with strong and electromagnetic decays of toponium can be used to our advantage to measure $\Gamma(t \to \text{all})$ through the chain:[36]

$$\Gamma(t \to \text{all}) = \left[\frac{\Gamma(t \to \text{all})}{\Gamma(t\bar{t} \to \text{all})}\right] \cdot \left[\frac{\Gamma(t\bar{t} \to \text{all})}{\Gamma(t\bar{t} \to \ell^+\ell^-)}\right] \cdot \Gamma(t\bar{t} \to \ell^+\ell^-) \quad . \tag{32}$$

The first factor is the fraction of weak t decays out of all toponium decays, the second is the inverse of the toponium leptonic branching ratio, and the third, the absolute width for toponium decay to $\ell^+\ell^-$, which can be obtained in the standard way by finding the area under the peak in the total cross section for toponium production in e^+e^- collisions. Using vertex detectors, one should also be able to verify that almost all t decays involve the transition $t \to b$. At the SSC, such a t quark is detectable in its semileptonic decays by using an "isolated lepton" cut.[29,30]

- $M_t > M_W$

In this case the t quark can decay into a real W with a width

$$\Gamma(t \to q_{-1/3} + W) = \frac{G_F}{8\pi\sqrt{2}} \frac{M_W^2(M_t^2 - M_W^2)^2}{M_t^3} \left(2 + \frac{M_t^2}{M_W^2}\right) \quad . \tag{33}$$

The width, being only first order in G_F, is much larger than one would obtain from (wrongly) extrapolating Eq. (31); for $M_t = 100$ GeV, the width is ≈ 80 MeV. It also grows asymptotically like M_t^3 rather than M_t^5.

In decays of the ground state T or $T^*(t\bar{q})$ mesons, individual exclusive channels should have very small branching ratios. In decays of heavy flavor mesons their branching ratios scale like $(f/M_Q)^2$, where f is a meson decay constant (like f_π or f_K), of order 100 MeV, and M_Q is the mass of the heavy quark. For D mesons individual channels have branching ratios of a few percent; for B mesons they are ten times smaller; and for T mesons they should be a hundred or more times smaller yet. It should be possible to treat T decays in terms of those of the constituent t quark, $t \to b + W^+$, with the b quark appearing in a b jet not so different than those already observed at PEP and PETRA.

There is one possible exception to these last statements, and that is when $M_t \approx M_b + M_W$. Then T and T^* will decay into a few exclusive channels with a real W plus a B, B^*, or slightly higher mass meson. If the W were a narrow resonance and M_t was slightly smaller than $M_b + M_W$, the $t \to b$ transition would be severely suppressed, allowing the $t \to s$ transition to be dominant in spite of its suppression by the KM factor, $|U_{ts}|^2$. However, the approximate 3 GeV width of the W smears out the threshold, allowing decays to B mesons through the lower tail of the W Breit–Wigner line shape even when $M_t \approx M_W$. The $t \to b$ transition is never suppressed by phase space compared to $t \to s$ by more than about[33] 30%.

Thus for $M_t > M_W$, the t quark is to be seen generally decaying into jets and discovered at TEV I or, if heavy enough, at the SSC. The production cross sections are discussed in the previous Section. The characteristic signature is obtained by looking for $t\bar{t}$ production from gluon fusion, with, say the W from the $\bar{t}$ decaying hadronically, $\bar{t} \to \bar{b} + W^- \to \bar{b}\bar{q}'q$, and the W from the t decaying leptonically, $t \to b + W^+ \to b\ell^+\nu_\ell$. The lepton should be isolated there being a missing momentum due to the neutrino, while both the $\bar{t}$ and t masses reconstruct within errors to the same value. The mass of the t quark can be determined from the momentum spectrum of the lepton relative to that of the b jet, or equivalently, as discussed in the last Section, the distribution in ΔR between the leptons from the W and the semileptonic decay of the b quark. It seems likely that in this way the gross properties of the t quark can be determined, but not much more.

ACKNOWLEDGEMENTS

REFERENCES

1. *Proceedings of the 1984 Snowmass Summer Study on the Design and Utilization of the Superconducting Super Collider*, edited by R. Donaldson and J. G. Morfin (American Physical Society, New York, 1984), referred to as SNOWMASS 84.

2. *Proceedings of the 1986 Summer Study on the Physics of the Superconducting Super Collider*, edited by R. Donaldson and J. Marx (American Physical Society, New York, 1987), referred to as SNOWMASS 86.

3. See D. Loveless *et al.* in $\bar{P}P$ *Options for the Supercollider*, edited by J. E. Pilcher and A. R. White (University of Chicago, Chicago, 1984), p. 294; J. W. Cronin *et al.*, SNOWMASS 84, p.161; B. Cox, F. J. Gilman, and T. D. Gottschalk, SNOWMASS 86, p. 33.

4. H. Albrecht *et al*, Phys. Lett. 192B, 245 (1987).

5. See, for example, B. L. Combridge, Nucl. Phys. B151, 429 (1979).

6. See, for example, the discussion in E. J. Eichten, I. Hinchliffe, K. Lane, and C. Quigg, Rev. Mod. Phys. 56, 579 (1984).

7. V. Gribov, E. M. Levin, and M. G. Ryskin, Phys. Rep. 101C, 1 (1982).

8. J. C. Collins, in *Supercollider Physics*, edited by D. Soper (World Scientific, Singapore, 1986), p. 62.

9. F. Olness and W.-K. Tung, in *Proceedings of the Workshop on From Colliders to Super Colliders*, Madison, Wisconsin, May 11–22, 1987, Int. Journal of Mod. Phys. A, 2, 1413 (1987).

10. Such a calculation is in progress by R. K. Ellis, S. Dawson, and P. Nason.

11. A. H. Mueller and P. Nason, Nucl. Phys. B266, 265 (1986).

12. This large factor arises from color factors and interference effects among the Feynman diagrams contributing to each process.

13. C. Albajar *et al.*, Phys. Lett. 186B, 237 (1987).

14. M. Aguilar–Benitez *et al.*, CERN preprint CERN–EP–87/45, 1987.

15. E. Berger, Argonne preprint ANL–HEP–PR–87–53, 1987 (unpublished).

16. F. Paige and S. Protopopescu, SNOWMASS 86, p. 320.

17. H.–U. Bengtsson and T. Sjostrand, Lund preprint LU–TP–87–3, 1987 and SNOW-MASS 86, p. 311.

18. The formalism discussed here closely follows I. I. Y. Bigi and A. I. Sanda, Nucl. Phys. B281, 41 (1987). We use the convention that the B_d meson has quark content $d\bar{b}$, while there is some switching from this definition in the above reference.

19. Other references to this and related topics include A. Pais and S. B. Treiman, Phys. Rev. D12, 2744 (1975); L. B. Okun *et al.*, Nuovo Cim. Lett. 13, 218 (1975); S. Barshay and J. Geris, Phys. Lett. 84B, 319 (1979); M. Bander *et al.*, Phys. Rev. Lett. 43, 242 (1979); A. B. Carter and A. I. Sanda, Phys. Rev. Lett. 45, 952 (1980) and Phys. Rev. D23, 1567 (1981); J. S. Hagelin, Nucl. Phys. B193, 123 (1981); J. Bernabeu and C. Jarlskog, Z. Phys. C8, 233 (1981); H. Y. Cheng, Phys. Rev. D26, 143 (1982); E. A. Paschos and U. Turke, Nucl. Phys. B243, 29 (1984); A. J. Buras, W. Slominski, and H. Steger, Nucl. Phys. B245, 369 (1984); L. Wolfenstein, Nucl. Phys. B246, 45 (1984); I. I. Y. Bigi and A. I. Sanda, Nucl. Phys. B193, 85 (1985); L. L. Chau and H. Y. Cheng, Phys. Lett. 165B, 429 (1985); I. Dunietz and J. L. Rosner, Phys. Rev. D34, 1404 (1986).

20. A. Pais and S. B. Treiman, ref. 19 and L. B. Okun *et al.*, ref. 19.

21. L. Wolfenstein, Phys. Rev. Lett. 51, 1945 (1983). Note that ρ in $\text{Im}\left(\frac{p}{q}\rho\right)$ is a ratio of amplitudes for B decay, and is not to be confused with the parameter (a pure, dimensionless number) in the Wolfenstein parametrization.

22. J. Bernabeu and C. Jarlskog, ref. 19.

23. L. L. Chau and H. Y. Cheng, ref. 19.

24. M. Bander *et al.*, ref. 19.

25. S. Barshay and J. Geris, ref. 19.

26. The utilization of the time dependence has been particularly emphasized by I. Dunietz and J. L. Rosner, ref. 19.

27. I. Wingerter, invited talk at the Topical Conference of the SLAC Summer Institute on Particle Physics, August 10–21, 1987 (unpublished).

28. J. Ellis, J. S. Hagelin, and S. Rudaz, Phys. Lett. 192B, 201 (1987); I. I. Y. Bigi and A. I. Sanda, Phys. Lett. 194B, 307 (1987); F. J. Gilman, invited talk at the International Symposium on the Fourth Family of Quarks and Leptons, Santa Monica, February 26 - 28, 1987 and SLAC-PUB-4315, 1987 (unpublished); G. Altarelli and P. J. Franzini, CERN preprint CERN-TH-4745/87, 1987 (unpublished); H. Harari and Y. Nir, SLAC preprint SLAC-PUB-4341, 1987 (unpublished); V. A. Khose and N. G. Uraltsev, Leningrad preprint, 1987 (unpublished); L. L. Chau and W. Y. Keung, UC Davis preprint UCD-87-02, 1987 (unpublished). J. F. Donoghue et al., SIN preprint SIN-PR-87-05, 1987 (unpublished); A. Ali, DESY preprint DESY-87/083, 1987 (unpublished); J. R. Cudell et al., University of Wisconsin preprint MAD/PH/353, 1987 (unpublished); A. Datta, E. A. Paschos, and U. Turke, Dortmund preprint DO-TH-87/9, 1987 (unpublished); D. Du and Z. Zhao, Phys. Rev. Lett. 59, 1072 (1987).

29. K. Lane and J. Rohlf, SNOWMASS 84, p. 737.

30. E. W. N. Glover and T. D. Gottschalk, SNOWMASS 86, p. 77.

31. G. Herten, these Proceedings.

32. F. Takasaki, invited talk at the 1987 International Symposium on Lepton and Photon Interactions at High Energies, Hamburg, July 27–31, 1987 (unpublished).

33. F. J. Gilman and R. Kauffman, unpublished.

34. I. I. Y. Bigi and H. Krasemann, Z. Phys. C7, 127 (1981).

35. F. Porter, invited talk at the International Symposium on the Fourth Family of Quarks and Leptons, Santa Monica, February 26–28, 1987 and Caltech preprint CALT–68–1434, 1987 (unpublished).

36. F. J. Gilman and H. F.-W. Sadrozinski, Mark II/SLC Working Group Note # 4–03, 1986 (unpublished).